Proceedings of the ASME 2013 Summer Heat Transfer Conference
HT2013
July 14-19, 2013, Minneapolis, Minnesota, USA

HT2013-17668 DRAFT

PHASE-CHANGE HEAT TRANSFER OF ETHANOL-WATER MIXTURES: TOWARDS DEVELOPMENT OF A DISTRIBUTED HYDROGEN GENERATOR

Manoj Kumar Moharana
Department of Mechanical Engineering
National Institute of Technology Rourkela
Rourkela-769008 (Odisha), India
moharanam@nitrkl.ac.in

Rohan M Nemade
Department of Mechanical Engineering
Indian Institute of Technology Kanpur
Kanpur-208016 (U.P.), India
rmnemade@iitk.ac.in

Sameer Khandekar
Department of Mechanical Engineering
Indian Institute of Technology Kanpur
Kanpur-208016 (U.P.), India
Phone: +91-512-259-7038, Fax: +91-512-259-7408, E-mail: samkhan@iitk.ac.in

ABSTRACT

Hydrogen fuel from renewable bio-ethanol is a potentially strong contender as an energy carrier. Its distributed production by steam reforming of ethanol on microscale platforms is an efficient upcoming method. Such systems require (a) a pre-heater for liquid to vapor conversion of ethanol water mixtures (b) a gas-phase catalytic reactor. We focus on the fundamental experimental heat transfer studies (pool and flow boiling of ethanol-water mixtures) required for the primary pre-heater boiler design. Flow boiling results (in a 256 μm square channel) clearly show the influence of mixture composition. Heat transfer coefficient remains almost constant in the single-phase region and rapidly increases as the two-phase region starts. On further increasing the wall superheat, heat transfer starts to decrease. At higher applied heat flux, the channel is subjected to axial back conduction from the single-phase vapor region to the two-phase liquid-vapor region, thus raising local wall temperatures. Simultaneously, to gain understanding of phase-change mechanisms in binary mixtures and to generate data for the modeling of flow boiling process, pool-boiling of ethanol-water mixtures has also been initiated. After benchmarking the setup against pure fluids, variation of heat transfer coefficient, bubble growth, contact angles, are compared at different operating conditions. Results show strong degradation in heat transfer in mixtures, which increases with operating temperature.

Keywords: Microchannel; Binary mixture; Heat transfer; Axial heat conduction; Flow boiling; Pool boiling.

INTRODUCTION

Ethanol-water mixtures are emerging to be of potential use in many applications, ranging from avionics cooling (Xie et al., (2005)), to the production of hydrogen by catalytic combustion (Ni et al. (2007)). Hydrogen fuel obtained from renewable bio-ethanol is a potentially strong contender as an energy carrier. Acknowledging the importance of distributed power devices on one hand, and microscale engineering on the other, we envisage developing an ethanol-based distributed hydrogen reactor system (~ 1 kW equivalent) using steam reforming. Such an integrated system requires a microscale pre-heater-boiler unit for converting the liquid water-ethanol mixtures to a gaseous state, for initiating the necessary catalytic reactions, as schematically shown in Fig. 1. The complete details of distributed hydrogen production process from bio-ethanol are discussed in Moharana et al. (2011).

Design of the pre-heater-boiler unit for the above process requires the knowledge of heat transfer coefficient of ethanol-water mixtures in microchannel geometries. Subsequently, development of generic mathematical models for flow boiling also requires basic data on pool boiling of ethanol-water mixtures. In this study we focus our attention on the experimental determination of heat transfer coefficient of these two fundamental processes, as applicable to ethanol-water mixtures, so that the design of the microchannel preheater-boiler required for distributed hydrogen production reactor, can be facilitated.

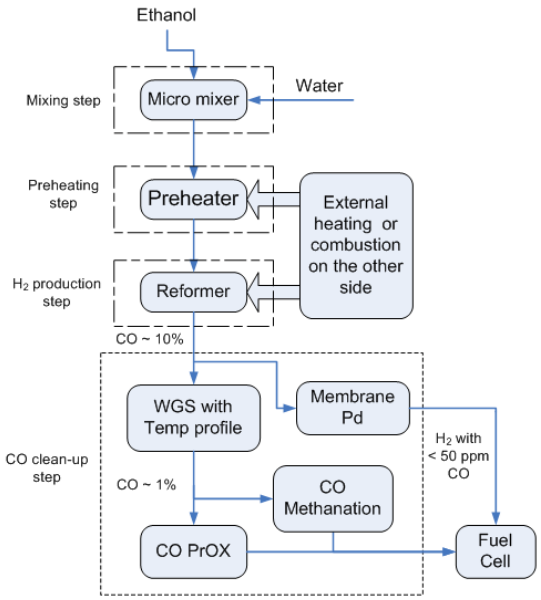

Figure 1: Schematic of an integrated reactor system for distributed generation of hydrogen from ethanol and water. Four major building units, (i) mixer (ii) preheater (iii) reformer and (iv) CO cleanup stages are required to develop an integrated reactor system (Moharana et al. (2011)).

Flow boiling of binary mixtures is more complicated than the corresponding pure fluids because (a) boiling point temperature varies with mixture composition for a given pressure (b) thermo-physical properties of the mixture do not follow linear mixing laws (c) the overall transport mechanism may be limited by the preferential mass transfer process of the less volatile component during phase-change, and (d) the bulk liquid contact angle, important for understanding boiling mechanism, usually shows highly non-linear behavior with varying concentration. The availability of literature on flow boiling of binary mixtures, other than refrigerants, especially in mini and microchannels, is rather sparse (Cheng and Mewes (2006); Moharana et al. (2011)).

In an early study, Peng et al. (1996) experimentally investigated subcooled flow boiling heat transfer characteristics of methanol-water mixtures in microchannels. Their findings suggest mixtures with small concentrations of the more volatile component augmented the flow boiling heat transfer while those with large concentrations reduced the heat transfer compared to pure methanol. This led to the conclusion that there exists an optimum concentration at which the flow boiling heat transfer reaches a maximum value. These characteristics were found to be affected by both liquid flow velocity and amount of subcooling. The heat transfer coefficient at the onset of flow boiling and in the partial nucleate boiling region was greatly influenced by liquid concentration, microchannel and plate configuration, flow velocity and amount of subcooling. However, microchannel size, flow velocity, mixture subcooling, and liquid concentration had no significant effect on heat transfer coefficient in fully developed nucleate boiling regime.

Peng and Peterson (1996) conducted experiments on subcooled flow boiling of methanol-water mixture in microchannels and found that the microchannel hydraulic diameter and aspect ratio significantly affected the fluid flow and heat transfer characteristics. They also found that for smaller mole fractions of the more volatile component (methanol), heat transfer was augmented, and reached the maximum value at a characteristic mole fraction. The experimental results also indicated that the augmented heat transfer region was extended with increase in mass flow rate through the microchannels.

Peng and Wang (1998, 2000) reviewed theoretical and experimental studies, for pure as well as fluid-mixtures, in boiling phase-change and transport phenomena in microchannels and microstructures, including bubble formation, phase transition and the fluid flow and heat transfer characteristics. Their investigations showed that flow boiling heat transfer of water, methanol, and their mixtures through rectangular and triangular microchannels display some unusual phenomena and characteristics. The experimental results showed that size and geometric configuration of microchannel, and mole fraction of water-methanol mixtures have a significant impact on the flow boiling, especially for nucleate boiling, and on bubble formation and growth in microchannels.

Xie et al. (2005) experimentally investigated flow and heat transfer characteristics of single-phase flow of 30% ethanol-water solution in microchannels and found that wall temperature has maximum influence on convection heat transfer. To the best of our knowledge, no investigation has presented the explicit effect of liquid concentration on the flow boiling heat transfer of ethanol-water mixtures.

Sun and Shi (2008) experimentally studied flow boiling of methanol-water binary mixture in rectangular microchannels having artificial cavities, subjected to an increasing heat flux condition. They found that boiling heat transfer is strongly influenced by the composition of working fluid. Sun and Shi (2008) also found that critical heat flux and heat transfer are enhanced under a low concentration of methanol due to the strong Marangoni effects.

Wu et al. (2009) experimentally studied single-phase flow and heat transfer characteristics of ethanol-water solution in trapezoidal silicon microchannels. They found that the volume concentrations had different effects on the flow friction and heat transfer. While the friction factor was only marginally affected by the change in the volume concentration (within the experimental band of error), there was considerable change in the heat transfer coefficient with the change in the concentration ratio of ethanol and water. The Nusselt number was found to be increasing with the increase of the volume concentration of ethanol.

Lin et al. (2011) experimentally studied convective boiling heat transfer of methanol-water mixture in a diverging microchannel with artificial cavities. They found that the critical heat flux increases slightly and then decreases as the concentration of methanol in the mixture is increased from

zero; the critical heat flux is maximum at mole fraction of ethanol ~ 0.3. They attributed this to Marangoni effect.

From the above discussions it is quite clear that only very limited number of experimental studies on flow boiling of binary mixtures in mini/microchannels exists in the open literature. Most existing studies are limited to single-phase flow of pure fluids only. No explicit heat transfer equation and flow pattern studies are available for binary mixtures, especially for the ethanol-water mixtures. In this background an experimental investigation is reported here to understand both the pool boiling and the forced convective heat transfer characteristics of ethanol-water binary mixtures in different proportions flowing through a horizontal microchannel having hydraulic diameter of 256 μm. For the flow boiling study, the fluid outlet temperature, heat flux and the heat transfer coefficient as a function of ethanol concentration in the mixture are evaluated.

EXPERIMENTAL DESCRIPTION

Both flow boiling and pool boiling of ethanol-water binary mixture are studied experimentally. The experimental facility developed for flow boiling is illustrated schematically in Fig. 2(b). A microchannel of length 68 mm is fabricated on stainless steel plate of size 76×7.8×1.5 mm^3 using laser micromachining, as shown in Fig. 2(a). The cross section of the microchannel is trapezoidal in shape with channel depth of 0.3 mm and channel widths of 0.35 mm and 0.25 mm. Thus, the hydraulic diameter of the microchannel is 0.256 mm. The working fluid flowing through the channel was heated electrically using a flexible silicon rubber thermofoil™ micro heater (make: Minco®) placed below the channel substrate. Metal-oxide filled silicone oil paste (heat sink compound having thermal conductivity of 2.9 W/mK) is used between the micro-heater and the microchannel substrate. It provides superior thermal conductivity for thermal coupling between the heater and the base of the microchannel substrate.

Low thermal conductive ceramic sheet is placed between the microheater and the backing plate to avoid heat loss from the bottom side of the microheater. Very low thermal conductive super-wool (0.08 W/mK at 200°C, 0.12 W/mK at 400°C), is used for insulating the entire test section cell. PFA insulated K-type micro-thermocouples (make: Omega®) with bead diameter 0.076 mm (model: 5SRTC-TT-K-40-72) are used for measuring both, fluid inlet/outlet and the channel wall temperatures. For measuring wall temperature along the channel length, six thermocouples are placed at equal intervals of 12 mm with the first thermocouple placed at a distance of 4 mm from the inlet of the microchannel, as shown. A differential pressure transducer (wet/wet type with built-in amplified output; 0 - 1 bar, 0 - 2 bar; Make: Honeywell®) is used for measuring the pressure drop across the microchannel length. The two ends of the differential pressure transducer are connected to the two respective inlet and outlet headers. National Instrument® make, 4 bit data acquisition thermocouple system (NI 9211) is used for measuring the thermocouple signal while the pressure signal is obtained via a 16-bit analog input module (NI-9205), using the Signal Express® GUI.

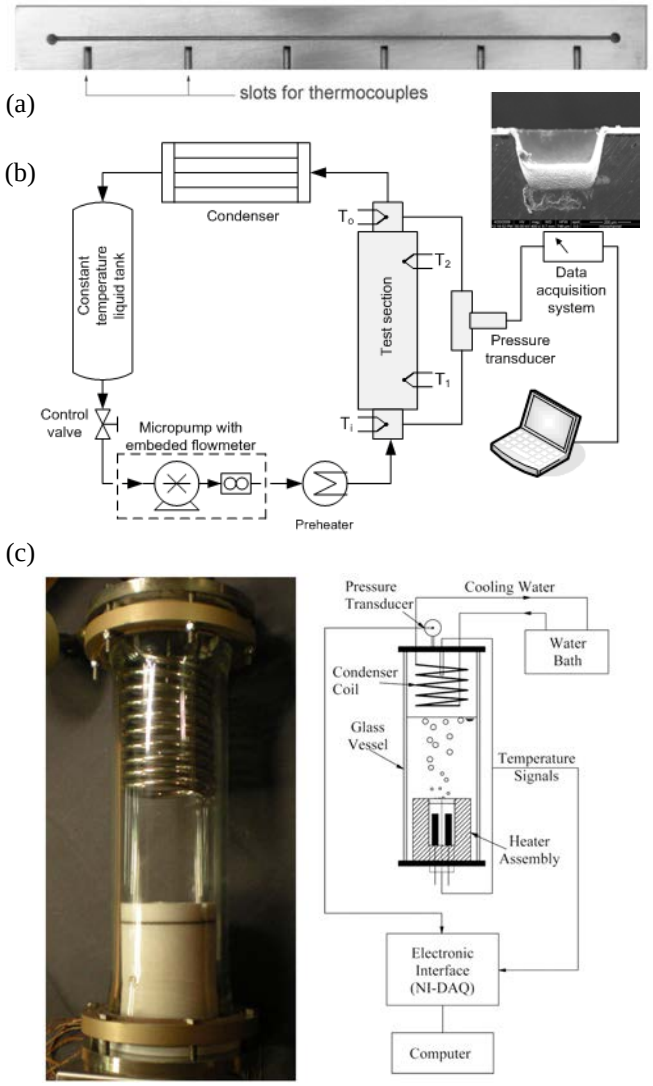

Figure 2: (a) Photograph of the microchannel with inset showing the cross section (b) Schematic layout of the experimental setup for flow boiling study, and, (c) Pool boiling study: photograph of the glass pressure vessel with heater assembly and schematic of the set-up.

The pool boiling setup is shown in Fig. 2 (c). Pool boiling was carried out on a 30 mm diameter interchangeable flat surface of aluminum and copper. The surface was heated from the bottom by four, 180 W cartridge heaters embedded in an aluminum cylinder, in thermal contact with the boiling surface. The heater assembly was surrounded by 15 mm thick solid Teflon insulation, as shown. The heater and the helical tube condenser assembly were mounted on the two sides of a cylindrical glass pressure vessel via Teflon seals, as shown, capable of maintaining vacuum better than 10^{-4} mPa. The condenser was supplied with cooling water at the desired temperature by a cryostat (Haake®). The bubble dynamics were captured by high speed camera (Photron®) at a frame rate of 2000 fps. The glass vessel was properly insulated from outside when videography was not being conducted. Five K-type thermocouples were mounted 1.0 mm below the boiling

surface, to provide average surface temperature. Also, one thermocouple each was employed for measuring the bulk liquid pool and vapor temperature. An absolute pressure transducer was mounted on the glass vessel to measure saturation pressure (Make: Honeywell, 0-3 bar abs.).

The heat flux at the boiling surface was estimated on the basis of the electrical power supplied and the boiling surface area (707 cm^2). This estimation was found to conform to heat flux estimated from a one-dimensional approximation through the heater block within 5%-7%.

RESULTS AND DISCUSSION

Flow boiling of ethanol-water binary mixture in microchannel is studied experimentally. Secondly, pool boiling of ethanol-water mixture is also carried out experimentally as described in previous section. In this section first flow boiling results are presented followed by pool boiling results.

(a) Flow Boiling of ethanol-water mixtures

For benchmarking, single-phase experiments are conducted for pure water, pure ethanol and their binary-mixtures. To verify the proper functioning of the flow loop, the single-phase pressure drop data are compared with the correlation proposed by Muzychka and Yovanovich (1998) for developing flow, as shown in Fig. 3. Several runs of experiments were conducted and the figure shows the consolidated results of all such experiments. In some of the runs, ethanol water mixtures were also used and the composite properties were then used for data-reduction. From Fig. 3., it is clear that the experimental pressure drops are within 10% of the theoretical correlation, as proposed by Muzychka and Yovanovich (1998).

Table 1 presents bubble point (T_b) and dew point (T_d) temperature of ethanol-water binary mixture in different proportions used in the experimental study. In all experimental runs, the value of T_b and T_d lies within ± 0.3°C of the theoretical values.

Next, the two-phase heat transfer data are discussed. The channel wall superheat is defined as

$$\Delta T_{sat} = T_w - T_{sat} \quad (1)$$

In present experimental condition, the average wall temperature T_w is calculated by taking the average of the wall temperature measured at six locations of the microchannel, as discussed earlier. Secondly, for the binary mixture working fluid the bubble point temperature (T_b) is considered as the saturation temperature (T_{sat}). In the single-phase flow region, the heat transfer coefficient is defined as,

$$h_{1\phi} = \frac{q''}{T_w - T_{fm}} \quad (2)$$

where T_{fm} is the mean of the fluid temperature at the inlet and at the outlet of the channel. In the two-phase flow region the heat transfer coefficient is defined as,

$$h_{2\phi} = \frac{q''}{T_w - T_{sat}} \quad (3)$$

Table 1: Bubble point temperature (T_b) and dew point temperature (T_d) of ethanol-water mixture.

Volume fraction of ethanol (y)	Mole fraction of ethanol (x)	T_b	T_d
0.0	0.000	100	100
0.2	0.071	87.5	98.0
0.4	0.174	83.7	95.0
0.6	0.316	81.4	90.5
0.8	0.550	79.0	82.4
1.0	1.000	78.2	78.2

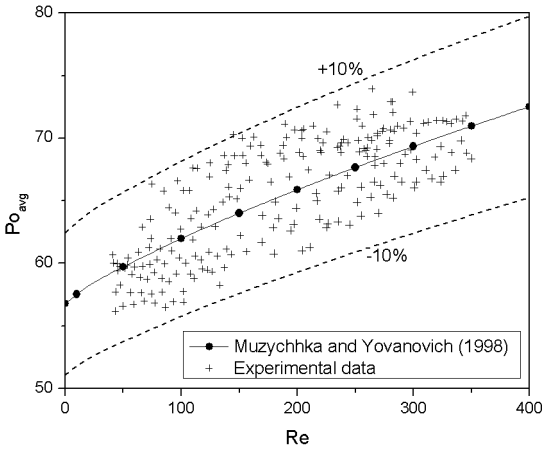

Figure 3: Pressure drop during single-phase flow as a function of flow Reynolds number (Re).

The performance of the microchannel test section can be best characterized quantitatively by its boiling curve, showing the appropriate system operating temperature as a function of the dissipated heat flux. The bulk fluid exit temperature and the channel wall temperature are measured as a function of wall heat flux (q"). Concentration of ethanol, in the mixture of water and ethanol at the inlet of the channel are varied. However, in all the experiments reported here, the net mass flux of the mixture is always kept constant at G = 299.2 kg/m^2.

Figure 4 shows the exit fluid temperature (T_{out}) as a function of average wall heat flux (q") for varying concentrations of ethanol (i.e. volume fraction of ethanol, y) in the mixture of ethanol-water at the inlet of the microchannel. The inlet fluid temperature is always maintained at 27 ± 3°C. The classical boiling plateau associated with latent heat transfer phenomenon of liquid-to-vapor phase-change is evident as the exit temperature remains almost constant in the range 78°C - 100°C, for different inlet concentrations of ethanol. Due to the limitation in maximum channel wall temperature the test section can survive (~114°C), the bulk fluid outlet temperature could not be raised to a level such that the fluid at the outlet will be single-phase vapor in all conditions.

Figure 5 depicts the wall superheat (T_w-T_{sat}) as a function of applied heat flux to the channel, at different volume fraction/mole fraction of ethanol at the channel inlet, at net mass flux of 299.2 kg/m^2s. The effect of mole fraction of ethanol on heat transfer can be observed in Fig. 5. In the single-phase region ((T_w-T_{sat}) < 0), for a given applied heat flux, the

wall superheat increases with increasing concentration of ethanol. The wall superheat is minimum for pure water and maximum for pure ethanol. In other words, for a certain value of wall superheat, the heat flux decreases with increase in molar fraction of ethanol in the mixture. The heat flux is maximum for pure water and minimum for pure ethanol. The decrease/increase in heat flux/wall superheat with varying composition of ethanol is not linear, as the thermo-physical property variation is quite non-linear between the two asymptotic composition limits of pure water and pure ethanol. As the bulk fluid temperature attains the bubble point temperature (T_b), the two-phase region starts and the value of heat flux increases rapidly near T_w-T_{sat} = 0, at a given super heat. In the two-phase region ((T_w-T_{sat}) > 0), the slope of the curve is higher compared to its slope in the single phase region.

This can be observed very prominently on a normal scale graph, which is not presented here. For the case of pure water two-phase could not be initiated within the channel length with the constraint of safe maximum wall temperature of the experimental setup.

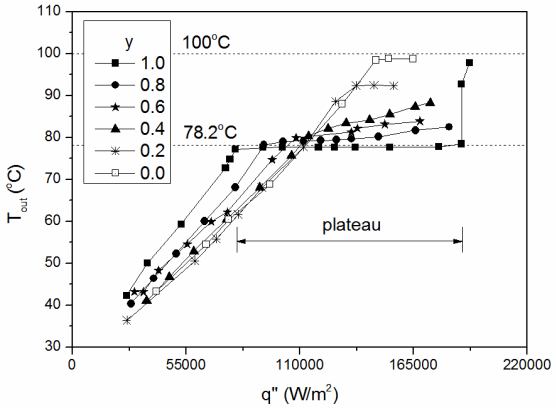

Figure 4: Bulk exit fluid temperatures as a function of the heat flux for varying concentrations of ethanol in the mixture of ethanol-water at the inlet of the channel.

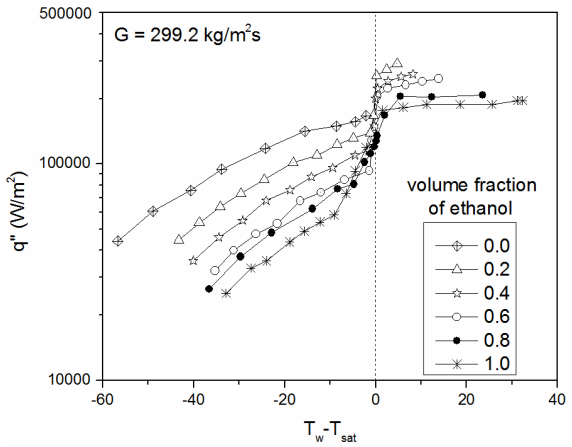

Figure 5: Variation of wall heat flux with wall superheat for ethanol-water mixture at different concentrations.

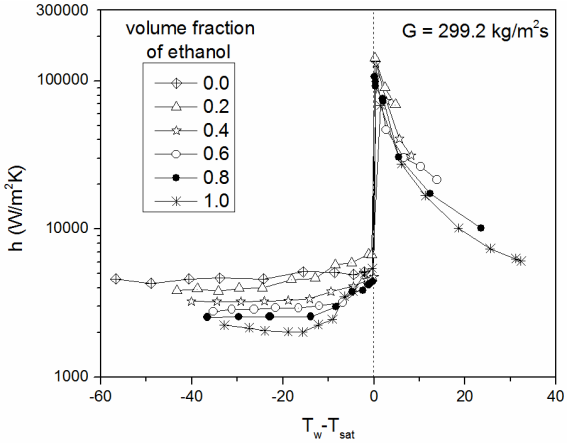

Figure 6: Heat transfer coefficient of ethanol-water mixture at different concentrations.

The heat transfer coefficient of the ethanol-water mixture as a function of ΔT_{sat} is shown in Fig. 6. The mass flux is G = 299.2 kg/m^{2}s. The heat transfer coefficient is calculated in the single-phase and the two-phase region as per the definitions in Eq. (2) and Eq. (3), respectively. The heat transfer coefficient is found to be almost constant in the single-phase region for a fixed composition of the mixture but it is found to be decreasing with increasing concentration of ethanol; maximum being for pure water and minimum being for pure ethanol. As the two-phase region starts, the heat transfer coefficient suddenly increases to a maximum and then decreases with further increase in the wall superheat.

(b) Axial conduction during subcooled flow boiling

In this section the importance of axial conduction in the substrate in a situation when flow boiling takes place inside a microchannel is highlighted. In a flow boiling situation several flow configurations are possible, and the effect of axial conduction varies with the particular flow conditions. For the purpose of analysis, and highlighting the effect of axial conduction in the substrate during an internal convective flow boiling situation with subcooled single-phase liquid entry and super-heated single-phase vapor exit, subjected to a constant heat flux boundary condition, the following cases are considered (a) Single-phase liquid region (sensible heating of liquid) (i) hydrodynamic and thermally developing flow region, (ii) fully developed region (b) Two-phase region (from onset of nucleate boiling to complete dry-out) (c) Single-phase vapor (sensible heating of vapor). In the single-phase liquid region the flow can be laminar or turbulent.

Correlations available in literature can be used to find the bulk fluid temperature and the tube wall temperature along the length of the tube. Figure 7 shows the variation of wall and bulk fluid temperature along the tube length with diameter D = 0.4 mm, inlet liquid flow Reynolds number = 100, heat flux = 20000 W/m^2, Bulk fluid temperature at tube inlet = 60°C. The vapor temperature at the outlet of the tube is 120°C for a tube length of 135 mm.

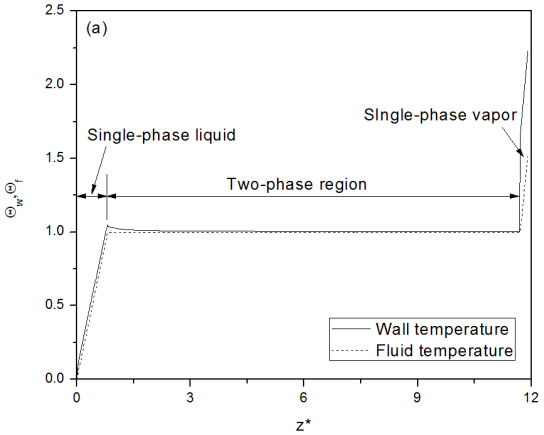

Figure 7: Axial variation bulk fluid and wall temperature of a circular tube subjected to constant heat flux boundary condition in a single-phase liquid, two-phase liquid-vapor, and single-phase vapor region.

Figure 7 is representative of the case when there is no axial conduction in the substrate, i.e., the conjugate effects are non-existent. The dimensionless bulk fluid temperature, wall temperature and axial length are defined as follows:

$$\Theta_f(z) = \frac{T_f(z) - T_i}{T_{sat} - T_i} \tag{4}$$

$$\Theta_w(z) = \frac{T_w(z) - T_i}{T_{sat} - T_i} \tag{5}$$

$$z^* = \frac{z}{Re \cdot Pr \cdot D} \tag{6}$$

where, T_i is the bulk fluid temperature at the inlet, T_{sat} is the saturation temperature of the fluid.

The presence of axial conduction in the microchannel during subcooled flow boiling where the flow along the channel is a combination of single-phase liquid, two-phase liquid-vapor, and single-phase vapor is experimentally studied. The variation of channel wall temperature along the length of the channel clearly indicates influence of axial conduction.

Figure 8 presents axial variation of fluid and channel wall temperature in the microchannel. As stated earlier the length of the channel is 68 mm and there are six micro thermocouples placed at x = 4, 16, 28, 40, 52, 64 mm away from the inlet of the channel to measure the channel wall temperature. The positions of the thermocouples are denoted by A, B, C, D, E, and F respectively, as shown in Fig. 8. The fluid temperatures at the channel inlet (T_{in}) i.e. x = 0 mm, and at the channel outlet (T_{out}) i.e. x = 68 mm are measured. In Fig. 8(a), the data are presented for pure ethanol having channel inlet temperature T_{in} = 24.5°C, for which the boiling point is 78.2°C, represented by a horizontal dotted line. For certain heat flux, the fluid outlet temperature T_{out} = 74.8°C. This indicates that the flow is single-phase throughout the length of the channel. The nature of the axial variation of the corresponding channel wall temperature is inline with the conventional theory, which is linear beyond the developing region.

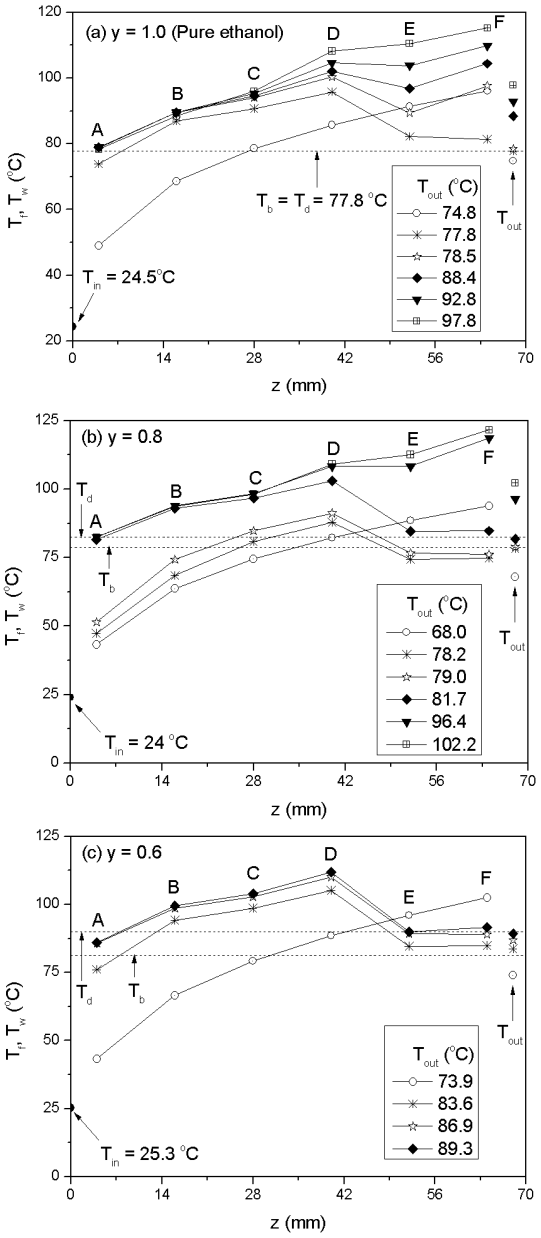

Figure 8: Axial variation of bulk fluid and channel wall temperature in the microchannel (a) pure ethanol (b) 80% ethanol by volume (c) 60% ethanol by volume.

Thus, the wall temperature at point F i.e. $T_{W\text{-}F}$ is maximum. On increasing the applied heat flux, the fluid outlet temperature increases to T_{out} = 77.8°C. This indicates that the flow is partly single-phase from the entry of the channel and it is two-phase liquid vapor in the remaining length of the channel. As discussed earlier, in a combined single-phase and two-phase fluid flow in a channel, the wall temperature is maximum towards the end of the single-phase region and it slightly decreases along the length of the channel in the two-phase region. This is exactly the same trend followed for T_{out} = 77.8°C which can be seen in Fig. 8(a). The wall temperature at the location D, i.e. $T_{W\text{-}D}$ is maximum. This indicates the single-

phase zone extends from the channel inlet to approximately up to location D, and beyond location D the flow is two-phase liquid vapor where $T_{w\text{-}E} < T_{W\text{-}D}$, and $T_{W\text{-}F} < T_{W\text{-}E}$.

As the applied heat flux is further increased, the fluid outlet temperature reaches T_{out} = 78.5°C which indicates that the fluid at the channel out let is single-phase vapor. Thus, the flow across the channel length is single-phase liquid at the entry of the channel, single-phase vapor towards the end of the channel, and two-phase liquid vapor in between the two single-phase regions. In such case the channel wall temperature increases along the channel length in the single-phase liquid region, decreases slightly in the two-phase region and again suddenly increases as the single-phase vapor region starts. This trend can be seen in Fig. 8(a) for T_{out} = 78.5°C. Thus, $T_{W\text{-}D} > T_{W\text{-}E}$, and $T_{W\text{-}E} < T_{W\text{-}F}$. The applied heat flux is increased further such that T_{out} = 97.8°C. The fluid at the channel outlet is superheated vapor. So the channel wall temperature in the single-phase vapor region will increase steeply. It is expected that there will be flow of heat in the solid substrate by means of axial back conduction from the single- phase vapor region to the two-phase liquid vapor region. This can be observed from the relative values of $T_{W\text{-}D}$, $T_{W\text{-}E}$, and $T_{W\text{-}F}$ where $T_{W\text{-}E} > T_{W\text{-}D}$. From the above discussion it can be concluded that at higher superheat of the vapor at the channel outlet there will be axial back conduction in the solid substrate. This will raise the wall temperature in the two-phase region such that the maximum wall temperature in the single-phase region will be less than the wall temperature in the two-phase region. In Fig. 8(a) it can be observed that with increasing heat flux the value of $T_{W\text{-}D}$ as well as $T_{w\text{-}E}$ are increasing but at lower heat flux $T_{W\text{-}D} > T_{W\text{-}E}$ and at higher heat flux $T_{W\text{-}D} < T_{W\text{-}E}$. This supports the above conclusion.

Figure 8(b) and 8(c) presents axial variation of channel wall temperature, and fluid inlet and outlet temperature for ethanol-water mixture having volume fraction of ethanol of 0.8, and 0.6 respectively. The trend observed in Fig. 8(b) and 8(c) are found to be same as it was observed in Fig. 8(a) for pure ethanol. For volume fraction of ethanol y = 0.6, experiment could not be conducted for fluid outlet temperature beyond 89.3°C due to limitation of the higher wall temperature that the present test section could sustain.

(c) Pool boiling of ethanol-water mixtures

The pool boiling experiments were carried out under controlled heat flux range of 0.01 MW/m^2 to 0.15 MW/m^2. The data reported here pertains to saturation temperature range of 30ºC to 50ºC. At each heat flux level, the average wall temperature was noted at steady state (the average of five surface mounted thermocouples). The wall superheat was then obtained as the difference between the average surface temperature and the bulk saturation temperature (measured by the thermocouple placed in the vapor space. Depending on the applied heat flux, the vapor space temperature was controlled by the temperature of the coolant water circuit passing through the condenser.

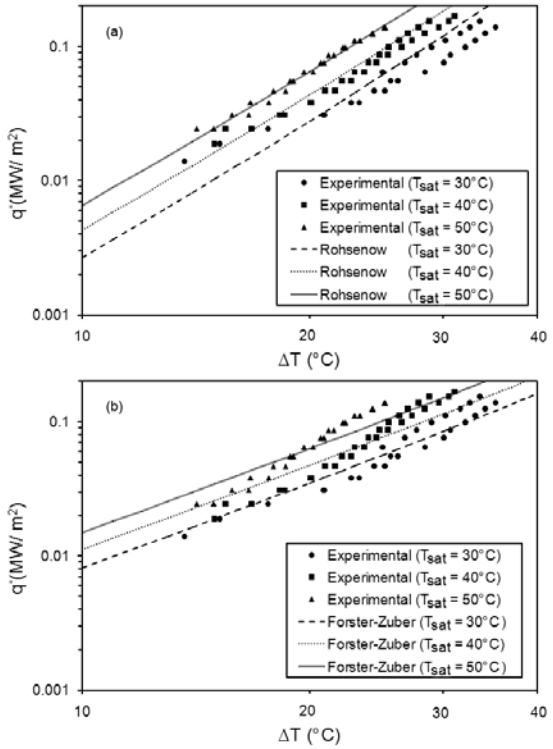

Figure 9: Benchmarking data set: comparison of heat flux versus wall superheat for pure water on aluminium surface at saturation temperatures for 30ºC, 40ºC and 50ºC, with two popular pool boiling correlations.

The pool boiling characteristics for water were first benchmarked with existing popular correlations for pure fluids, i.e. Rohsenow correlation and Forster-Zuber correlation (Carey (2007)). Figure 9 shows comparison of the obtained experimental data with these two correlations, respectively (For the Rohsenow correlation the surface constant C_{sf} has been taken to be equal to 0.022). The experimental results were found to conform to correlations with a maximum deviation of 16 %.

In addition, high speed videographic images of individual bubbles were captured at 2000 fps, for pure water at low pressures, as shown in Fig. 10. As expected from classical bubble growth mechanisms, the growth is rapid initially, in the inertia controlled regime, wherein the bubble remained nearly hemispherical in shape. Subsequently, the bubble spread on the surface stops as the buoyant forces overcome the surface tension. As buoyant forces become dominant the bulk of bubble shifts upwards even as the base of the bubble sticks to the surface causing necking. Images post detachment indicated considerable reflux of liquid into the vapor bubble from the bottom as the interface that was stretched just before detachment, rebounded into the bubble, due to the surrounding liquid gushing from below. The volume of the bubble at several stages of its growth was estimated by image processing considering the bubble interface to be a part of solid of revolution. Thereafter, the equivalent spherical volume can be estimated.

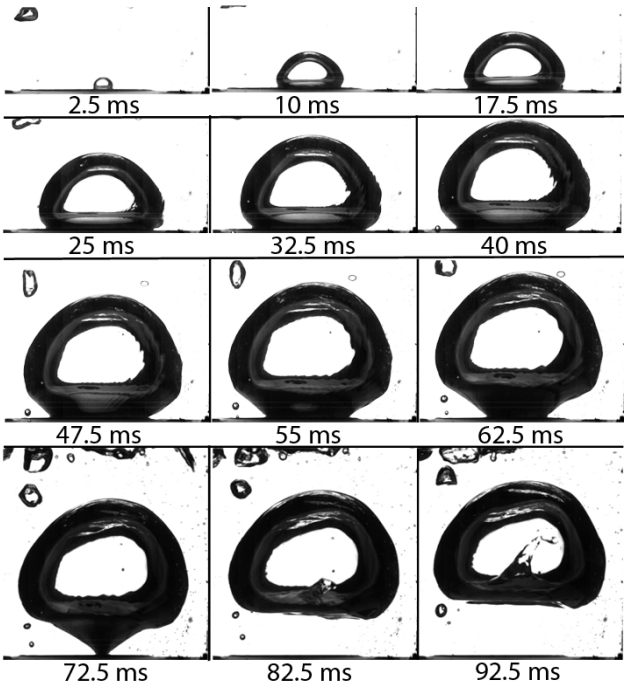

Figure 10: Bubble growth and departure dynamics for pure water at T_{sat} = 50°C, q" = 0.046 MW/m^2.

Figure 11 shows a representative result of above image analysis method of T_{sat} = 50°C, q" = 0.046 MW/m^2, for both pure water and 2% molar ethanol-water mixture (= 6.25% v/v). It was observed that the bubble departure size was reduced in case of the mixture. While, the growth rate in the inertia controlled regime is similar, it is clear that the latter part of the growth gets severely hampered by the mass transfer limitation of the more volatile component, i.e. ethanol (Carey (2007)). In addition, the final departure diameter for the mixture is also smaller than that of pure water which is attributed to considerable change in mixture properties even at low concentration of ethanol (Moharana et al. (2011)). It may be noted that for the same vapor saturation temperature, the system pressure is higher in the case of mixtures.

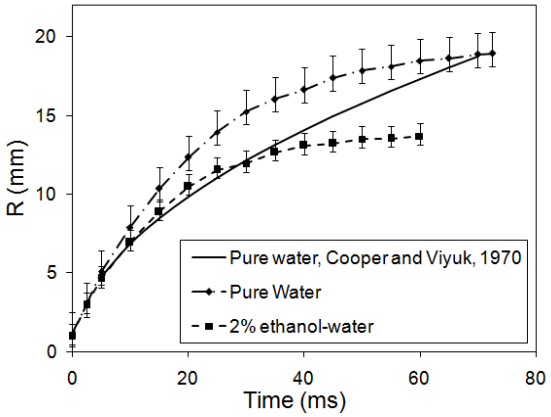

Figure 11: Bubble growth comparison for pure water and mixture for T_{sat} = 50°C, q" = 0.046 MW/m^2.

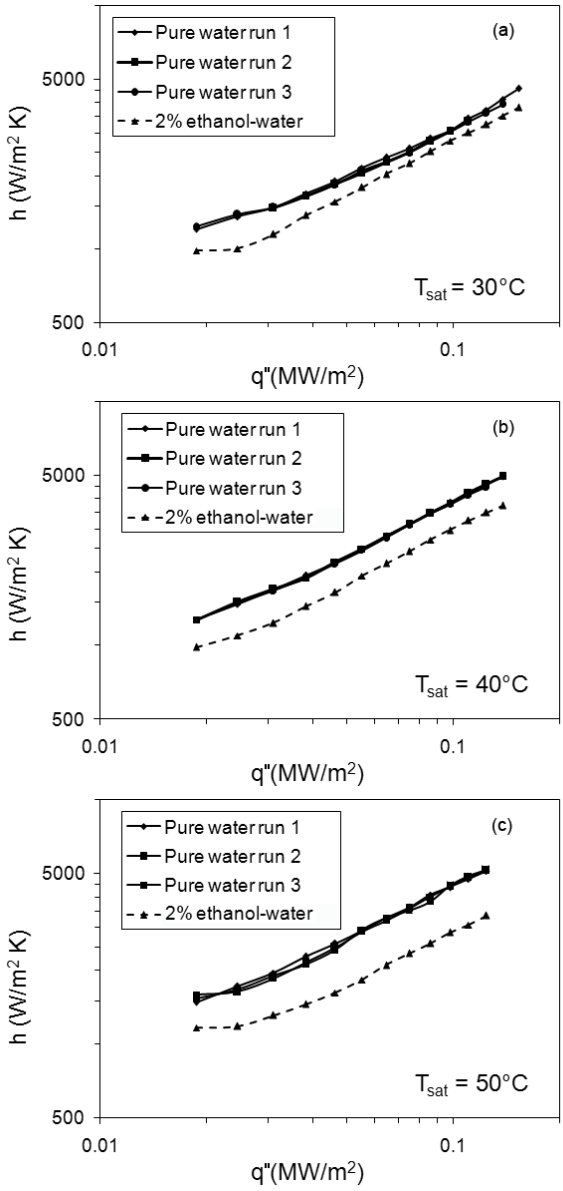

Figure 12: Heat transfer coefficient v/s heat flux data for pure water and 2% ethanol-water mixture at different operating temperatures.

The heat transfer coefficient for pool boiling was defined as,

$$h = \frac{q''}{\Delta T} \tag{7}$$

The heat transfer coefficients for 2% molar ethanol-water mixture were found to be less than that of pure water at all operating temperatures that were considered, over entire range of heat flux conditions. This reduction in heat transfer coefficient was found to be more significant as the operating temperature increased, as can be seen in Fig. 12. The reduction in heat transfer coefficient can be related as described above to the differential concentration of the respective liquids between bulk and close to the bubble interface. The reduction in concentration at the interface locally raises the saturation

temperature, hence requiring a higher wall temperature. This essentially raises the wall superheats in relation to bulk saturation temperature, for a given heat flux.

In addition, the temporal variation of average contact angle was also measured from the images for several bubble sets. Figure 13 shows this data for both pure water and mixture for T_{sat} = 50°C. Initially as the bubble is almost hemispherical, the contact angle is high. Then as the bubble grows rapidly over the surface, the liquid surrounding the bubble is pushed away. This receding of the liquid over the surface reduces the contact angle much like the receding contact angle of a drop moving on a surface. Eventually, as the bubble volume becomes sufficient enough for buoyant forces to become dominant, the bubble spreading action on the surface stops; the bubble starts moving upwards. Thereafter, the contact angle remains constant as necking occurs, until departure.

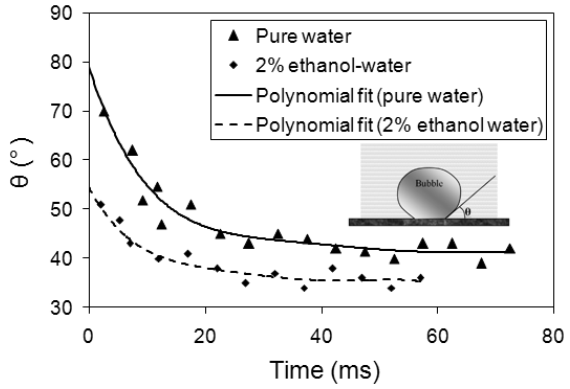

Figure 13: Variation of contact angle of the bubble interface during bubble growth from the heated surface.

SUMMARY AND CONCLUSION

The design of the preheater-boiler to be employed in the distributed hydrogen production using steam reforming requires the knowledge of heat transfer coefficient of ethanol-water mixtures during flow boiling in microchannels. In addition, pool boiling data for mixtures is also required for fundamental understanding of the transport phenomena. Experimental results for flow boiling of ethanol water mixtures in a wide range of mixture composition have been provided. The heat transfer coefficient remains almost constant in the single-phase region and suddenly increases as the two-phase region starts. On further increasing the wall superheat the heat transfer starts to decrease. The possible effect of axial back conduction in microchannels is also highlighted. The pool boiling data indicated deterioration in heat transfer coefficient even at small concentration of ethanol in water. Mixtures also led to smaller bubble departure diameters and considerably low growth rate in the latter part of the bubble growth process. This is attributed to mass transfer limitations imposed by the more volatile component. Presently, further detailed investigation is ongoing to estimate the effect of operating temperature as well as composition on the boiling characteristics of ethanol water mixtures, under flow and pool boiling conditions.

ACKNOWLEDGMENTS

This work is funded by the Department of Science and Technology, Government of India, under the IIT Kanpur sponsored Project No: DST/CHE/20060304, titled 'Micro-devices for Process Applications'.

NOMENCLATURE

C_{sf}	surface constant (-)
D	Diameter (m)
G	mass flux (kg/m^{2}s)
h	heat transfer coefficient (W/m^{2}K)
Po	Poiseuille number (=f·Re)
Pr	Prandtl number (-)
q"	heat transfer rate (W/m^2)
R	bubble radius (m)
Re	Reynolds number (-)
T	Temperature (ºC or K)
x	axial distance (m), mole fraction of ethanol (-)
y	volume fraction of ethanol (-)
z	axial length (m)
z*	dimensionless axial length (= x/Re·Pr·D_h)

Symbols

Θ	dimensionless temperature (-)
θ	contact angle (º)
ΔT	temperature difference (ºC or K)

Subscript

avg	average
b	bubble point
d	dew point
f	fluid
fm	mean fluid
i	inlet, inner
in	inlet
m	mean
max	maximum
out	outlet
sat	saturation
w	wall
z	axial location, local value
1ϕ	single-phase
2ϕ	two-phase

REFERENCES

Carey V.P., 2007, Liquid-Vapor Phase-Change Phenomena, 2nd ed., Taylor and Francis.

Cheng L., Mewes D., 2006, “Review of two-phase flow and flow boiling of mixtures in small and mini channels,” Int. J. Multiphase Flow, 32(2), pp. 183–207.

Cooper M.G., Vijuk R.M., 1970, “Bubble growth in nucleate pool boiling”, in: Proceedings of the Fourth International Heat Transfer Conference, Elsevier, Paris-Versailles, pp. 1–11.

Lin P.H., Fu B.R., Pan C., 2011, “Critical heat flux on flow boiling of methanol-water mixtures in a diverging microchannel with artificial cavities,” Int. J. Heat Mass Transfer, 54(15-16), pp. 3156–3166.

Muzychka Y.S., Yovanovich M.M., 1998a, “Modeling friction factors in non-circular ducts for developing laminar flow,” 2nd AIAA Theoretical Fluid Mech. Meet., Albuquerque, USA.

Moharana M.K., Peela N.R., Khandekar S., Kunzru D., 2011, “Distributed hydrogen production from ethanol in a microfuel processor: Issues and challenges,” Renewable and Sustainable Energy Reviews, 15(1), pp. 524–533.

Ni M., Leung D.Y.C., Leung M.K.H., 2007, “A review on reforming bio-ethanol for hydrogen production,” International Journal of Hydrogen Energy, 32(15), pp. 3238–3247.

Peng X.F., Peterson G.P., 1996 “Forced convection heat transfer of single-phase binary mixtures through microchannels,” Exp. Therm. Fluid Science, 12(1), pp. 98–104.

Peng X.F., Peterson G.P., Wang B.X., 1996, “Flow boiling of binary mixtures in microchanneled plates,” International Journal of Heat and Mass Transfer, 39(6), pp. 1257–1264.

Peng X.F., Wang B.X., 1998, “Forced-convection and boiling characteristics in microchannels,” In: 11th Int. Heat Transfer Conference. pp. 371-390 (vol. 1), Kyongju, Korea.

Peng X.F., Wang B.X., 2000, “Nucleation and thermodynamic non-equilibrium for boiling in microchannels and microstructures,” Ann. Rev. Heat Transf., 11, pp. 307–350.

Sun C.L., Shi M.S., 2008, “Marangoni effects on the flow boiling of methanol/water mixtures in microchannels,” in: Proc. 19th Int. Symp. Transport Phenomena, Reykjavik, Iceland.

Wu H., Wu X., Wei Z., 2009, “Flow friction and heat transfer of ethanol-water solutions through silicon microchannels,” J. Micromechanics and Microengineering, 19(4), pp. 1–10.

Xie Y.Q., Yu J.Z., Zhao Z.H., 2005, “Experimental investigation of flow and heat transfer for the ethanol-water solution and FC-72 in rectangular microchannels,” Heat and Mass Transfer, 41(8) 695–702.